Non-linear growth-temperature relationship leads to opposite responses to warming in cold versus warm populations

Max Lindmark[1,*], Jan Ohlberger[2,3,*], and Anna Gårdmark[1]

[1]Department of Aquatic Resources, Swedish University of Agricultural Sciences, Uppsala, Sweden

[2]School of Aquatic and Fishery Sciences, University of Washington, Seattle, WA 98195, USA

[3]Washington Department of Fish and Wildlife, 1111 Washington St. SE, Olympia, WA 98501, USA

Authorship: *Shared first-authorship, correspondence to max.lindmark@slu.se

Keywords: climate change, body growth, size, fish, non-linear, temperature-size rule, von Bertalanffy, Sharpe-Schoolfield, perch, spatiotemporal

Abstract

Body size is a key trait that has been declining in many biological assemblages, partly due to within-species changes in individual growth rates and mean body size attributed to climate warming. Yet, robust tests of warming-effects in natural populations are scarce due to a lack of long time series with large temperature contrasts. We compiled length-at-age data for Eurasian perch (*Perca fluviatilis*) from 10 populations along the Baltic Sea coast between 1953–2015 (23605 individuals). By fitting von Bertalanffy growth curves to individual length-at-age trajectories, we estimated growth-temperature relationships across large ranges of environmental temperature. We identify a non-linear relationship between growth and temperature, but find little evidence for local adaptation in thermal response curves. Cold populations show a positive response whereas warm populations show a negative response to increasing temperatures. Understanding population-specific effects of warming on growth and size is critical for predicting climate impacts to species and ecosystems.

Introduction

Body growth is an individual-level trait that is relevant to ecology across all levels of biological organisation (Barneche *et al.* 2019, Peters 1983). In aquatic systems in particular, body growth is sensitive to environmental conditions, is related to individual fitness (Sibly *et al.* 2018), determines species interactions and dictates how much energy is transferred between trophic levels (Lindeman 1942). It is also directly related to body size, which is a key ecological trait (Peters 1983) that is correlated with diet, survival and reproductive success (Barneche *et al.* 2018) and largely shapes size-dependent species interactions (Ursin 1973, Werner and Gilliam 1984).

In ectotherms such as fish, environmental temperature has a large influence on body growth via the effects on metabolic rate (Jobling 1997, Brown *et al.* 2004). For species living at temperatures cooler than that which maximizes growth, as commonly observed (Lindmark *et al.* 2022, Tewksbury *et al.* 2008), a slight increase in temperature is likely to be beneficial to growth. Body growth or size-at-age of fish in natural environments, is commonly observed to correlate positively with temperature, especially for small or young fish (Huss *et al.* 2019, Lindmark *et al.* 2023, Baudron *et al.* 2014, Thresher *et al.* 2007, Oke *et al.* 2022). The effects on old fish, however, often are smaller or negative (Ikpewe *et al.* 2020, Morrongiello *et al.* 2014, van Dorst *et al.* 2019), although there are exceptions (Lindmark *et al.* 2023) and responses can vary within populations, e.g., with sex (van Dorst *et al.* 2023). Experimental and modelling studies have pointed to that size-dependent responses of growth and size could be due to optimum growth temperatures being lower for larger fish (Lindmark *et al.* 2022), or that warming is linked to earlier maturation, after which energy is increasingly allocated to reproduction over somatic growth (Wootton *et al.* 2022, Niu *et al.* 2023), or both (Audzijonyte *et al.* 2022). In natural systems, other factors such as competition and food limitation also influence growth directly (Ohlberger *et al.* 2023, Oke *et al.* 2020, Cline *et al.* 2019), and indirectly by reducing the optimal growth temperatures (Brett 1971, Brett *et al.* 1969, Huey and Kingsolver 2019). To understand fish responses to changing temperatures, it is therefore important to evaluate growth-temperature relationships in natural systems, and across gradients of environmental temperature.

The ability to quantify the impacts of temperature change on growth and size, or other ecological traits, is often limited by relatively short time series that contain small temperature contrasts (White 2019, Freshwater *et al.* 2023). As an alternative, studies often use space-for-time approaches

(van Dorst *et al.* 2019, van Denderen *et al.* 2020, Morrongiello *et al.* 2014) to estimate the effects of temperature on growth. However, it is difficult to know to what extent we can infer effects of warming in a given location from the temperature effects estimated across locations over a limited time (Perret *et al.* 2024). Both the estimates (van Denderen *et al.* 2020) and the form of the growth-temperature relationship may differ. For example, responses to warming tend to be unimodal, whereas they can be more linear or exponential across all populations of a species (van Denderen *et al.* 2020). For projecting impacts of warming at the species level, another missing piece is to understand the extent of local adaptation to the experienced thermal environments (Eliason *et al.* 2011). That is, to what extent populations conform to a global species-wide thermal performance curve, versus having developed local thermal response curves with population-specific optima. Testing this requires time series with large temperature contrasts both within and between multiple populations in the wild.

Here, we seek to understand how climate warming is affecting the growth of freshwater fish, using *Perca fluviatilis*, hereafter perch, as a case study. Perch is a widely distributed, non-commercially exploited fish with a stationary lifestyle that is common along the Swedish Baltic Sea coast, which makes it an ideal species for analyzing effects of temperature change on growth across environmental gradients. Specifically, we quantify growth-temperature relationships from 10 populations and evaluate if there is support for site-specific temperature-optima for growth, or if all populations' response curves can be mapped onto a global growth-temperature relationship. To address this question, we collated size-at-age data from back-calculated growth-trajectories for 23 605 individual fish over seven decades, and fit statistical models relating cohort-specific growth estimates to reconstructed temperatures.

Methods

Data

We compiled individual-level size-at-age from perch and sea surface temperature data from 10 sites along the Swedish Baltic Sea coast. The longest time series started in 1953 and the shortest in 1985, and the average time series length was 34 years, which can be compared to an average generation time of 6 years (Froese and Pauly 2010) (Fig. 1). The temperature contrast in this data set is

great both within each site and across sites (Fig. 2), due to long time series and a large latitudinal gradient. Also contributing to the large temperature range is the inclusion of sites artificially heated by warm water discharge from nearby nuclear power plants (sites (SI_HA and BT in Fig. 2). The size-at-age data include information on age (at catch), total length (at catch, in millimetres), sex, and back-calculated length-at-age (in millimetres). Back-calculated length-at-age was derived from annuli rings on the operculum bones (part of the gill lid), with control counts of age done on otoliths (ear stones). This method is common in fisheries (Essington *et al.* 2022, Morrongiello and Thresher 2015), and is based on an assumed power-law relationship between the distance of annuli rings and fish length (Thoresson 1996), which allows reconstruction of the individual's body length at each age when annuli rings where formed. Individual-level data originate from different fish monitoring programs using gill-nets. Individuals sampled for age and growth were selected from the total catch from the gill net survey in each site using random or length-stratified sub-sampling of the catch, but information on stratification method could not be retrieved for all data.

We reconstructed local temperatures at each fishing site using three types of temperature data: automatic temperature loggers deployed near the fishing sites, manually measured temperatures at the time of fishing, and extended reconstructed sea surface temperature, ERRST (Huang *et al.* 2017). We chose these three types because they are complementary. Logger data provide daily temperatures during the ice-free season but do not go back as far in time as the growth data. Temperatures at the fishing event give a snapshot temperature at the site, and go back as far in time as we have fishing data. However, temperatures during fishing may not be representative of the whole growth season, and since we work with back-calculated length-at-age, we also need temperatures for years prior to fishing. Therefore, we also used modelled temperature time series (ERRST), which both provide good seasonal coverage and extend far back in time, but have a much coarser spatial resolution than the other sources. These three temperature data sources overlap in time (Fig. S6), which allowed us to standardize the data using a statistical model (see next section).

Statistical analyses

To characterise individual growth rates, we fit von Bertalanffy growth equations (von Bertalanffy 1938) to the multiple observations of back-calculated length-at-age for each individual using non-

linear least squares:

$$L_t = L_\infty(1 - e^{-k \cdot age}), \tag{1}$$

where L_t is the size [mm] at age t [years], L_∞ the asymptotic size [mm], and k is the von Bertalanffy "growth" coefficient [year^{-1}]. It describes the time it takes to reach the asymptotic size, and is hence not a growth rate *per se* (which has unit size per time), but is often used as a proxy for it. We only used length-at-age, meaning only length at a back calculated integer age (i.e., length at the formation of the age-ring), because sampling has occurred in different times of the year. We fit this model to every individual age 5 or older to ensure enough data points per individual to reliably fit the model. The filtering resulted in 142 023 data points across 23 605 individuals. We then calculated the median k by cohort and site across individuals (resulting in $n = 306$ k values) (Fig. 1).

In order to relate the site- and cohort-specific growth coefficients to temperature over time, we reconstructed average annual temperature sea surface temperature (sst) for each site using generalized additive models assuming Student-t distributed residuals to account for extreme observations:

$$sst_i \sim \text{Student-t}(\mu_i, \phi, \nu) \tag{2}$$

$$\mu_i = \alpha_t + f(day) + source \tag{3}$$

where μ_i is the mean sst, ϕ is the scale and ν is the degrees of freedom parameter. ν was not estimated within the model, but found by iteratively testing different values and visually inspecting QQ-plots to see how well the model could capture the heavy tails in the data. We used two sets of values, $\nu = 6$ for sites BS (Brunskär), BT (Biotest), FB (Finbo), FM (Forsmark), MU (Muskö), RA (Råneå) and SI_EK (Simpevark Ekö) and $\nu = 10$ for HO (Holmön), JM (Kvädöfjärden), and SI_HA (Simpevarp Hamnefjärden) (Fig. S7). The parameter α_t is the mean sst of year t (included as factor), $f(day)$ is a global smooth implemented as a penalized cyclic spline (i.e., the ends match—in this case December 31st and January 1st) for the effect of day-of-the-year, and source is the mean temperature for each temperature source. We fit the temperature models by site separately, because the presence of artificial heating from nuclear power plants warranted complicated inter-

actions between time, source and site in a global model, and those models did not converge. We fit our models in R version 4.2.3 (R Core Team 2020) using the R package `sdmTMB` (Anderson *et al.* 2022, 2021) (version 0.3.0.9002), which uses `mgcv` (Wood 2017) to implement penalized smooths as random effects, and `TMB` (Kristensen *et al.* 2016) to estimate parameters via maximum marginal likelihood and the Laplace approximation to integrate over random effects.

We assessed convergence by confirming that the maximum absolute gradient with respect to all fixed effects was < 0.001 and that the Hessian matrix was positive-definite. We evaluated fit by visually inspecting QQ-plots (Fig. S7) of randomized quantile residuals based on MCMC draws (Anderson *et al.* 2022, Rufener *et al.* 2021) (Fig. S7). From these models, we predicted daily temperatures (Figs. S8, S9) (for the "logger" level) and then averaged these across year to acquire a covariate to be used to the cohort-specific von Bertalanffy growth coefficients (Fig. 2).

To estimate how von Bertalanffy growth coefficients were related to temperature we used the Sharpe-Schoolfield model (Schoolfield *et al.* 1981, Padfield *et al.* 2020), which can be viewed as an extension of the Arrhenius equation to account also for deactivation of rates with temperature. We used a mixed-effects version of it to allow site-specific parameters (as we were interested in local temperature optima), assuming Student-t distributed residuals to account for extreme observations:

$$k_i \sim \text{Student-t}(\mu_{j[i]}, \phi, \nu) \tag{4}$$

$$\mu_i = \frac{k_{0_j} e^{E_j(\frac{1}{kT_c} - \frac{1}{kT})}}{1 + e^{E_{h_j}(\frac{1}{kT_{h_j}} - \frac{1}{kT})}} \tag{5}$$

$$k_{0_j} \sim \text{N}(\mu_{k_{0_j}}, \sigma_{k_{0_j}}) \tag{6}$$

$$E_j \sim \text{N}(\mu_{E_j}, \sigma_{E_j}) \tag{7}$$

$$E_h \sim \text{N}(\mu_{E_h}, \sigma_{E_h}) \tag{8}$$

$$T_{h_j} \sim \text{N}(\mu_{T_{h_j}}, \sigma_{T_{h_j}}) \tag{9}$$

where $\mu_{j[i]}$ is the mean for site j, ϕ is the scale and ν is the degrees of freedom parameter. In equation 5, k_0 is the growth coefficient at the reference temperature T_C (here set to 8°C), E_j [eV] is the activation energy, E_{h_j} [eV] characterises the decline in the rate past the peak temperature, and T_{h_j} [°C] is the temperature at which the rate is reduced to half of the rate it would have in

the absence of deactivation due to high temperatures. We fit the model in a Bayesian framework. This allows us to fit site-varying parameters, and to use informative priors. Since we use a mechanistic model describing the temperature dependence of biological rates, we defined priors based on probable values of these parameters and their constraints. To ensure our priors were reasonable, we conducted prior predictive checks (Fig. S1) (Wesner and Pomeranz 2021), which is the prediction of the model using only the prior. We also evaluated prior versus posterior distributions and summaries of these (Fig. S2), and conducted sensitivity analyses with respect to our choice of priors (Fig. S3). After this procedure, we ended up with the following normal priors: $\mu_{k_{0_j}} \sim \mathrm{N}(0.3, 0.5)$, $\mu_{E_j} \sim \mathrm{N}(0.8, 1)$, $\mu_{E_h} \sim \mathrm{N}(2, 1)$, and $\mu_{T_{h_j}} \sim \mathrm{N}(10, 5)$, for the population-level parameters. The priors were truncated to be positive. All distributional parameters (σ) were given the same Student-t$(0, 2.5, 3)$ prior. To compare local, site-specific Sharpe-Schoolfield curves and their optimum temperatures with a global curve, we also fitted a pooled Sharpe-Schoolfield model where parameters did not vary by site. We used the same set of priors for the mixed (on the population level parameters) and the pooled model. This was done to evaluate whether the deviation from the global optimum could be explained by temperature. The models were fit using the R package `brms` (Bürkner 2018, 2017). We used 4000 iterations and 4 chains. Model convergence and fit were assessed by ensuring potential scale reduction factors were close to 1, suggesting all four chains converged to a common distribution (Gelman *et al.* 2003), as well as by visually inspecting QQ-plots based on Bayesian probability residuals, calculated as in the `tidybayes` R package (Kay 2019) and posterior predictive checks (Fig. S4).

Results

We find large inter-annual fluctuations in annual average temperatures between sites, and increasing trends over time in some sites (Fig. 2). Due to the spatial and temporal range of data, and the artificial heating from nuclear power plant cooling water, we observe large contrasts in average temperatures, which were not clearly related to latitude (Fig. 1). Across all sites, mean annual average temperatures range from 4°C–16°C, and the largest range within a site (over time) is 6°C–16°C (site BT). In some sites and years, this means temperatures exceeded the predicted optimum

growth temperature from the pooled model (Fig. 2). Individual growth trajectories of fish showed large variation within and across sites (Fig. 3).

Our results show that site-specific Sharpe-Schoolfield curves align well with the pooled (global) temperature-dependence curve (Fig. 4). This means that in general, populations in relatively cold sites show positive relationships of body growth with temperature, whereas populations in relatively warm sites show negative relationships with temperature, but all conform to an overall "global" temperature-dependence. Furthermore, negative impacts of temperature on growth rate are largely found as a result of artificial warming, although some sites with warming due to climate change have the highest observed temperatures around the predicted optimum, suggesting that further warming would no longer increase growth in these sites. The global predictions show that the growth coefficients are similar at the coldest (4°C) and the warmest temperatures (16°C), with an overall optimum around 9°C (Fig. 4). Hence, we observe only a minor asymmetry in the growth curve, where the steepness of the curve is slightly larger at above- compared to below-optimum temperatures.

We find that 6 of 10 sites have median temperature optima within the 95% credible intervals of the pooled model, although all site-specific optimum temperatures overlap in their uncertainty intervals with the pooled optimum temperature (Fig. 5). Importantly, while there is some variation among sites in the estimated optimum growth temperature, this variation is not systematically related to temperature (Fig. 5), as would have been the prediction if perch in the different sites had adapted their growth rate to be maximized in the experienced environmental conditions.

Discussion

We show that population-specific growth-temperature curves map closely onto a pooled 'global' growth-temperature curve across all populations, and that residual variation in estimated population-specific thermal optima of body growth is not systematically related to local environmental temperatures. We thus find no evidence for local adaptation of growth variation with temperature, despite considerable differences in the average temperatures that these populations experience in their natural environment. Our results instead suggest that populations in relatively cold environments will benefit from climate warming via increased body growth rates up to a certain 'global'

temperature optimum, whereas populations in relatively warm environments will experience reduced growth due to the negative effects of warming beyond their optimum growth temperature.

In line with our results, Neuheimer *et al.* (2011) found that for populations of banded morwong (*Cheilodactylus spectabilis*), increasing temperatures were associated with reduced growth rates for the population at the warm edge of the species' distribution (New Zealand) but higher growth rates for populations at the colder edge of the range (Tasmania). Similarly, Morrongiello and Thresher (2015) found that body growth of tiger flathead in populations off Southeast Australia increased with temperature but not in the warmest area. Analogously, English *et al.* (2022) found that groundfish in the Northeast Pacific often responded positively to warming if they were in cool locations, and negatively if they were in warm locations (where both biomass and temperature change were expressed as velocities). These and our findings illustrate the importance of testing for population-specific temperature-sensitivities when studying species responses to warming, and of accounting for both the rate of climate change and the baseline temperature conditions.

This growth-temperature pattern arises due to an absence of local thermal adaptation in growth. The ability to adapt to local environmental conditions allows populations to expand their range and better cope with spatially varying environmental conditions (Kirkpatrick and Barton 1997). Changes in trait-temperature relationships due to thermal adaptation in natural populations are expected in response to climate warming (Angilletta 2009), and previous studies have shown that local adaptation in physiological traits can facilitate different thermal optima among populations (e.g., Atlantic cod, Righton *et al.* (2010)). However, adaptive capacities and the pace of thermal adaptation differ among species (Martin *et al.* 2023) and depend on life-history trade-offs, heritability, underlying genetic variation, the potential for gene flow (Kirkpatrick and Barton 1997), and environmental conditions. The apparent lack of contemporary thermal adaptation in Baltic Sea perch, despite low gene flow between populations due to limited dispersal and movement (Bergek and Björklund 2009), indicates limitations in evolutionary changes to local temperature. This suggests that similar factors may also limit future thermal adaptation that would allow local populations to better withstand changing temperatures. A low adaptive capacity implies that body growth rates in populations already experiencing temperatures around or above their thermal optimum will decline with further warming. This will likely result in lower biomass production in

warm environments, as observed, for example, across spatial temperature gradients (van Dorst *et al.* 2019).

Our study also illustrates the importance of accounting for unimodal temperature dependencies. Often simpler models like the exponential Arrhenius equation are used to model biological and ecological processes (e.g., Vasseur and McCann (2005), Savage *et al.* (2004), Lindmark *et al.* (2018)), under the assumption that the 'biologically relevant temperature range' which species occupy is below their optimum. However, across all areas, we find that as many as 40% of all data points (growth coefficients, k) are above the estimated site-specific optimum (35% if omitting sites with an artificially extended temperature range due to nuclear power plants). This echoes the point raised many times (e.g., Englund *et al.* (2011)), that exponential temperature dependencies may be of limited use. Growth rates are only exponentially related to temperature even further from the optimum, i.e., below the inflection point of the unimodal curve. We therefore recommend researchers to consider that temperatures close to the optimum may in fact be biologically relevant, in which case models other than the Arrhenius equation are more appropriate.

There are a number of limitations to our analysis. For instance, growth in temperate regions varies over the year and it is therefore difficult to know which temperature variable that is best to use to relate to cohort-specific growth coefficients. Given also that growing season lengths differ in our data set due to different light conditions, we opted to use a simple annual average. Degree days (the integral of time above a certain temperature threshold) is an often recommended metric (Neuheimer and Grønkjær 2012), but there is some uncertainty in temperatures below which growth does not occur, even for a well studied species like perch (Karås and Thoresson 1992), and whether or not that varies between sites. Lastly, it is not straightforward to formally test for differences in thermal optimum between populations, and we mainly base our interpretation on the lack of systematic variation in site-specific optimum temperatures for growth, which appear to not be related to the average temperature at each site.

In summary, our findings suggest that annual mean temperatures are either approaching or have surpassed optimum growth temperatures for the populations examined here (Figs. 2 and 5). Our ability to detect this pattern relies heavily on the length of the time series as well as the unusually large temperature contrasts due to warm water pollution from nuclear power plants, which highlights the importance of long term environmental monitoring across environmental

gradients. Considering the lack of evidence for recent local adaptation to temperature, we expect that adverse effects of continued warming on Baltic Sea perch will accumulate and decrease both individual and population growth rates in these populations. Similar constraints on adaptive capacities in response to warming can be expected for other species of fish, and ectotherms more generally.

Acknowledgements

We are very grateful to all the staff involved in data collection over the years and to the funding bodies of the long-term monitoring. The study was financed by the Swedish Research Council Formas (grant no. 2023-2026 to Max Lindmark) and SLU Quantitative Fish- and Fisheries Ecology.

Author contributions

All authors contributed to the manuscript. A.G. conceived the study, M.L. and A.G. prepared the raw data and J.O. contributed to preparing temperature data. J.O. and M.L. led the design with contributions from AG. M.L and J.O conducted the statistical analyses. All authors conceptualized the results, contributed to revisions, and gave final approval for publication.

Data Availability Statement

All code and data to reproduce the results are available on GitHub (https://github.com/maxlindmark/perch-growth), and will be deposited on Zenodo before publication.

References

Anderson, S.C., Ward, E.J., English, P.A. and Barnett, L.A.K. (2022) sdmTMB: An R package for fast, flexible, and user-friendly generalized linear mixed effects models with spatial and spatiotemporal random fields. *bioRxiv (https://doi.org/10.1101/2022.03.24.485545)* , 2022.03.24.485545.

Anderson, S.C., Ward, E.J., Barnett, L.A.K. and English, P.A. (2021) sdmTMB: Spatiotemporal species distribution GLMMs with 'TMB'.

Angilletta, M.J. (2009) *Thermal Adaptation: A Theoretical and Empirical Synthesis*. Oxford University Press.

Audzijonyte, A., Jakubavičiūtė, E., Lindmark, M. and Richards, S.A. (2022) Mechanistic Temperature-Size Rule Explanation Should Reconcile Physiological and Mortality Responses to Temperature. *The Biological Bulletin* **243**, 220–238.

Barneche, D.R., Jahn, M. and Seebacher, F. (2019) Warming increases the cost of growth in a model vertebrate. *Functional Ecology* **33**, 1256–1266.

Barneche, D.R., Robertson, D.R., White, C.R. and Marshall, D.J. (2018) Fish reproductive-energy output increases disproportionately with body size. *Science* **360**, 642–645.

Baudron, A.R., Needle, C.L., Rijnsdorp, A.D. and Marshall, C.T. (2014) Warming temperatures and smaller body sizes: Synchronous changes in growth of North Sea fishes. *Global Change Biology* **20**, 1023–1031.

Bergek, S. and Björklund, M. (2009) Genetic and morphological divergence reveals local subdivision of perch (Perca fluviatilis L.). *Biological Journal of the Linnean Society* **96**, 746–758. URL https://doi.org/10.1111/j.1095-8312.2008.01149.x.

Brett, J.R., Shelbourn, J.E. and Shoop, C.T. (1969) Growth rate and body composition of fingerling sockeye salmon, *Oncorhynchus nerka*, in relation to temperature and ration size. *Journal of the Fisheries Research Board of Canada* **26**, 2363–2394.

Brett, J.R. (1971) Energetic responses of salmon to temperature. A study of some thermal relations in the physiology and freshwater ecology of sockeye salmon (*Oncorhynchus nerka*). *Integrative and Comparative Biology* **11**, 99–113.

Brown, J.H., Gillooly, J.F., Allen, A.P., Savage, V.M. and West, G.B. (2004) Toward a metabolic theory of ecology. *Ecology* **85**, 1771–1789.

Bürkner, P.C. (2017) **Brms** : An *R* Package for Bayesian Multilevel Models Using *Stan*. *Journal of Statistical Software* **80**.

Bürkner, P.C. (2018) Advanced Bayesian Multilevel Modeling with the R Package brms. *The R Journal* **10**, 395–411.

Cline, T.J., Ohlberger, J. and Schindler, D.E. (2019) Effects of warming climate and competition in the ocean for life-histories of Pacific salmon. *Nature Ecology & Evolution* **3**, 935–942.

Eliason, E.J., Clark, T.D., Hague, M.J., Hanson, L.M. *et al.* (2011) Differences in thermal tolerance among sockeye salmon populations. *Science* **332**, 109–112.

English, P.A., Ward, E.J., Rooper, C.N., Forrest, R.E. *et al.* (2022) Contrasting climate velocity impacts in warm and cool locations show that effects of marine warming are worse in already warmer temperate waters. *Fish and Fisheries* **23**, 239–255.

Englund, G., Öhlund, G., Hein, C.L. and Diehl, S. (2011) Temperature dependence of the functional response. *Ecology Letters* **14**, 914–921.

Essington, T.E., Matta, M.E., Black, B.A., Helser, T.E. and Spencer, P.D. (2022) Fitting growth models to otolith increments to reveal time-varying growth. *Canadian Journal of Fisheries and Aquatic Sciences* **79**, 159–167.

Freshwater, C., Duguid, W., Juanes, F. and McKinnell, S. (2023) A century-long time series reveals large declines and greater synchrony in Nass River sockeye salmon size-at-age. *Canadian Journal of Fisheries and Aquatic Sciences* **80**, 1098–1109.

Froese, R. and Pauly, D. (2010) FishBase.

Gelman, A., Carlin, JB., Stern, HS. and Rubin, DB. (2003) *Bayesian Data Analysis. 2nd Edition.* Chapman and Hall/CRC, Boca Raton.

Huang, B., Thorne, P., Banzon, V.F., Boyer, T. *et al.* (2017) NOAA Extended Reconstructed Sea Surface Temperature (ERSST), Version 5. NOAA National Centers for Environmental Information.

Huey, R.B. and Kingsolver, J.G. (2019) Climate warming, resource availability, and the metabolic meltdown of ectotherms. *The American Naturalist* **194**, E140–E150.

Huss, M., Lindmark, M., Jacobson, P., van Dorst, R.M. and Gårdmark, A. (2019) Experimental evidence of gradual size-dependent shifts in body size and growth of fish in response to warming. *Global Change Biology* **25**, 2285–2295.

Ikpewe, I.E., Baudron, A.R., Ponchon, A. and Fernandes, P.G. (2020) Bigger juveniles and smaller adults: Changes in fish size correlate with warming seas. *Journal of Applied Ecology* **58**, 847–856.

Jobling, M. (1997) Temperature and growth: Modulation of growth rate via temperature change. In: *Global Warming: Implications for Freshwater and Marine Fish*, volume 61 (eds. C.M. Wood and D.G. McDonald). Cambridge University Press, Cambridge, pp. 225–254.

Karås, P. and Thoresson, G. (1992) An application of a bioenergetics model to Eurasian perch (Perca fluviatilis L.). *Journal of Fish Biology* **41**, 217–230.

Kay, M. (2019) Tidybayes: Tidy Data and Geoms for Bayesian Models.

Kirkpatrick, M. and Barton, N.H. (1997) Evolution of a Species' Range. *The American Naturalist* **150**, 1–23.

Kristensen, K., Nielsen, A., Berg, C.W., Skaug, H. and Bell, B.M. (2016) TMB: Automatic Differentiation and Laplace Approximation. *Journal of Statistical Software* **70**, 1–21.

Lindeman, R.L. (1942) The Trophic-Dynamic Aspect of Ecology. *Ecology* **23**, 399–417.

Lindmark, M., Huss, M., Ohlberger, J. and Gårdmark, A. (2018) Temperature-dependent body size effects determine population responses to climate warming. *Ecology Letters* **21**, 181–189.

Lindmark, M., Karlsson, M. and Gårdmark, A. (2023) Larger but younger fish when growth outpaces mortality in heated ecosystem. *eLife* **12**, e82996.

Lindmark, M., Ohlberger, J. and Gårdmark, A. (2022) Optimum growth temperature declines with body size within fish species. *Global Change Biology* **28**, 2259–2271.

Martin, R.A., da Silva, C.R.B., Moore, M.P. and Diamond, S.E. (2023) When will a changing climate outpace adaptive evolution? *WIREs Climate Change* **14**, e852.

Morrongiello, J.R. and Thresher, R.E. (2015) A statistical framework to explore ontogenetic growth variation among individuals and populations: A marine fish example. *Ecological Monographs* **85**, 93–115.

Morrongiello, J.R., Walsh, C.T., Gray, C.A., Stocks, J.R. and Crook, D.A. (2014) Environmental change drives long-term recruitment and growth variation in an estuarine fish. *Global Change Biology* **20**, 1844–1860.

Neuheimer, A.B., Thresher, R.E., Lyle, J.M. and Semmens, J.M. (2011) Tolerance limit for fish growth exceeded by warming waters. *Nature Climate Change* **1**, 110–113.

Neuheimer, A.B. and Grønkjær, P. (2012) Climate effects on size-at-age: Growth in warming waters compensates for earlier maturity in an exploited marine fish. *Global Change Biology* **18**, 1812–1822.

Niu, J., Huss, M., Vasemägi, A. and Gårdmark, A. (2023) Decades of warming alters maturation and reproductive investment in fish. *Ecosphere* **14**, e4381.

Ohlberger, J., Cline, T.J., Schindler, D.E. and Lewis, B. (2023) Declines in body size of sockeye salmon associated with increased competition in the ocean. *Proceedings of the Royal Society B: Biological Sciences* **290**, 20222248.

Oke, Krista.B., Cunningham, C.J., Westley, P.a.H., Baskett, M.L. *et al.* (2020) Recent declines in salmon body size impact ecosystems and fisheries. *Nature Communications* **11**, 4155.

Oke, K.B., Mueter, F.J. and Litzow, M.A. (2022) Warming leads to opposite patterns in weight-at-age for young versus old age classes of Bering Sea walleye pollock. *Canadian Journal of Fisheries and Aquatic Sciences* .

Padfield, D., Castledine, M. and Buckling, A. (2020) Temperature-dependent changes to host–parasite interactions alter the thermal performance of a bacterial host. *The ISME Journal* **14**, 389–398.

Perret, D.L., Evans, M.E.K. and Sax, D.F. (2024) A species' response to spatial climatic variation does not predict its response to climate change. *Proceedings of the National Academy of Sciences* **121**, e2304404120.

Peters, R.H. (1983) *The Ecological Implications of Body Size*, volume 2. Cambridge University Press.

R Core Team (2020) *R: A Language and Environment for Statistical Computing*. Vienna, Austria.

Righton, D.A., Andersen, K.H., Neat, F., Thorsteinsson, V. *et al.* (2010) Thermal niche of Atlantic cod Gadus morhua: Limits, tolerance and optima. *Marine Ecology Progress Series* **420**, 1–13.

Rufener, M.C., Kristensen, K., Nielsen, J.R. and Bastardie, F. (2021) Bridging the gap between commercial fisheries and survey data to model the spatiotemporal dynamics of marine species. *Ecological Applications* **31**, e02453.

Savage, V.M., Gillooly, J.F., Brown, J.H., West, G.B. and Charnov, E.L. (2004) Effects of Body Size and Temperature on Population Growth. *The American Naturalist* **163**, 429–441.

Schoolfield, R.M., Sharpe, P.J.H. and Magnuson, C.E. (1981) Non-linear regression of biological temperature-dependent rate models based on absolute reaction-rate theory. *Journal of Theoretical Biology* **88**, 719–731.

Sibly, R.M., Kodric-Brown, A., Luna, S.M. and Brown, J.H. (2018) The shark-tuna dichotomy: Why tuna lay tiny eggs but sharks produce large offspring. *Royal Society Open Science* **5**, 180453.

Tewksbury, J.J., Huey, R.B. and Deutsch, C.A. (2008) Putting the Heat on Tropical Animals. *Science* **320**, 1296–1297.

Thoresson, G. (1996) Metoder för övervakning av kustfiskbestånd (in Swedish). Technical Report 3, Kustlaboratoriet, Fiskeriverket, Öregrund.

Thresher, R.E., Koslow, J.A., Morison, A.K. and Smith, D.C. (2007) Depth-mediated reversal of the effects of climate change on long-term growth rates of exploited marine fish. *Proceedings of the National Academy of Sciences, USA* **104**, 7461–7465.

Ursin, E. (1973) On the prey size preferences of cod and dab. *Meddelelser fra Danmarks Fiskeri-og Havun- dersgelser* **7:8598**.

van Denderen, D., Gislason, H., van den Heuvel, J. and Andersen, K.H. (2020) Global analysis of fish growth rates shows weaker responses to temperature than metabolic predictions. *Global Ecology and Biogeography* **29**, 2203–2213.

van Dorst, R.M., Gårdmark, A., Kahilainen, K.K., Nurminen, L. *et al.* (2023) Ecosystem heating experiment reveals sex-specific growth responses in fish. *Canadian Journal of Fisheries and Aquatic Sciences* .

van Dorst, R.M., Gårdmark, A., Svanbäck, R., Beier, U., Weyhenmeyer, G.A. and Huss, M. (2019) Warmer and browner waters decrease fish biomass production. *Global Change Biology* **25**, 1395–1408.

Vasseur, D.A. and McCann, K.S. (2005) A mechanistic approach for modelling temperature-dependent consumer-resource dynamics. *The American Naturalist* **166**, 184–198.

von Bertalanffy, L. (1938) A quantitative theory of organic growth (inquiries on growth laws. II). *Human Biology* **10**, 181–213.

Werner, E.E. and Gilliam, J.F. (1984) The ontogenetic niche and species interactions in size-structured populations. *Annual Review of Ecology and Systematics* **15**, 393–425.

Wesner, J.S. and Pomeranz, J.P.F. (2021) Choosing priors in Bayesian ecological models by simulating from the prior predictive distribution. *Ecosphere* **12**, e03739.

White, E.R. (2019) Minimum Time Required to Detect Population Trends: The Need for Long-Term Monitoring Programs. *BioScience* **69**, 40–46.

Wood, N., S. (2017) *Generalized Additive Models: An Introduction with R.* 2nd edition. CRC/Taylor & Francis.

Wootton, H.F., Morrongiello, J.R., Schmitt, T. and Audzijonyte, A. (2022) Smaller adult fish size in warmer water is not explained by elevated metabolism. *Ecology Letters* **25**, 1177–1188.

Figures

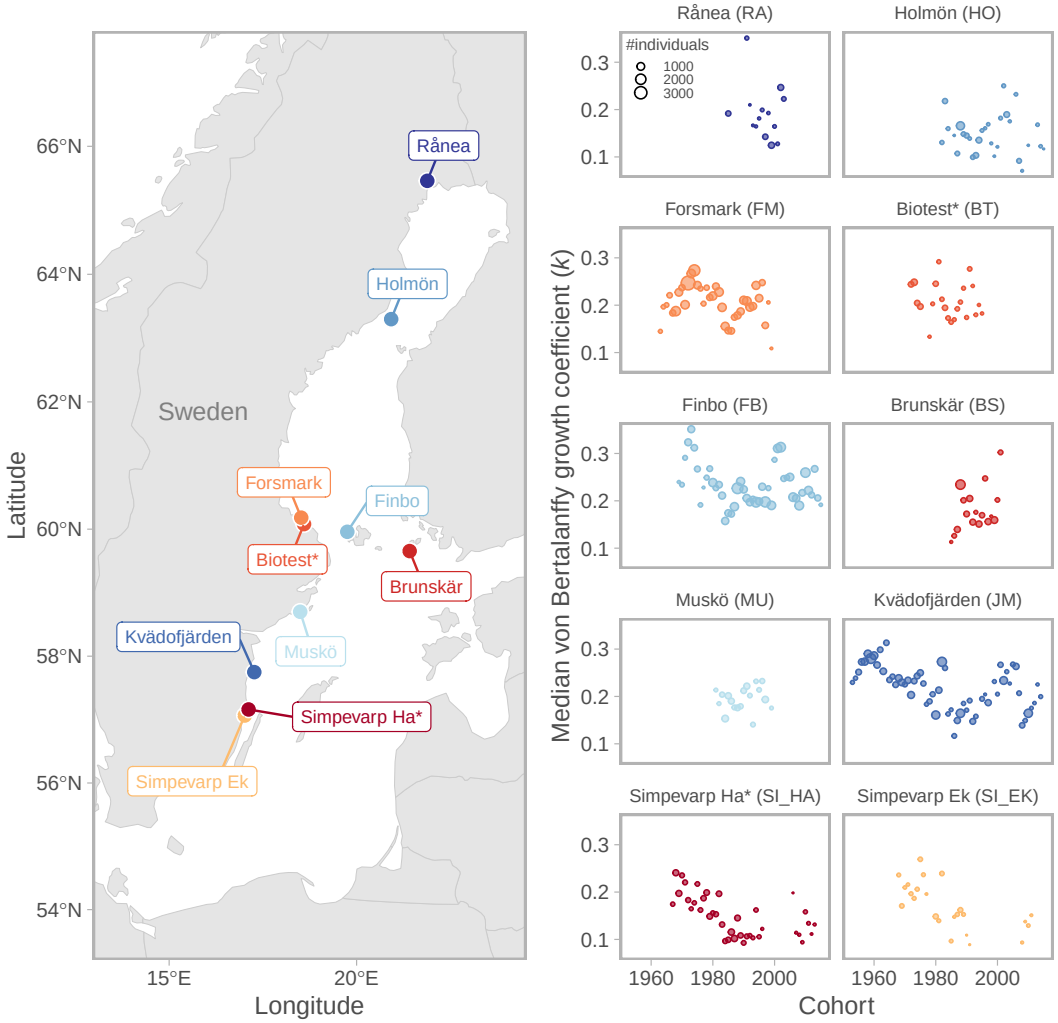

Figure 1: Map of sampling locations (left) and time series of the median von Bertalanffy growth coefficients by cohort (right), where colours are assigned based on the minimum temperature in the growth time series, ranging from blue (coldest) to red (warmest). Circle size corresponds to the number of individuals in that cohort and site.

Figure 2: Annual average sea surface temperature as predicted by the GAM-model fitted to three temperature sources. Colour indicates temperature. The solid red horizontal line depicts the median optimum temperature, calculated from 10.000 draws from the expectation of the posterior predictive distribution from the Sharpe-Schoolfield model fitted to all sites pooled, and the dashed red horizontal lines depict the 5^{th} and 95^{th} percentile of the same distributions of optimum temperatures. Areas SI_HA and BT have been heated by warm water discharge from nuclear power plants since 1972 and 1980, respectively.

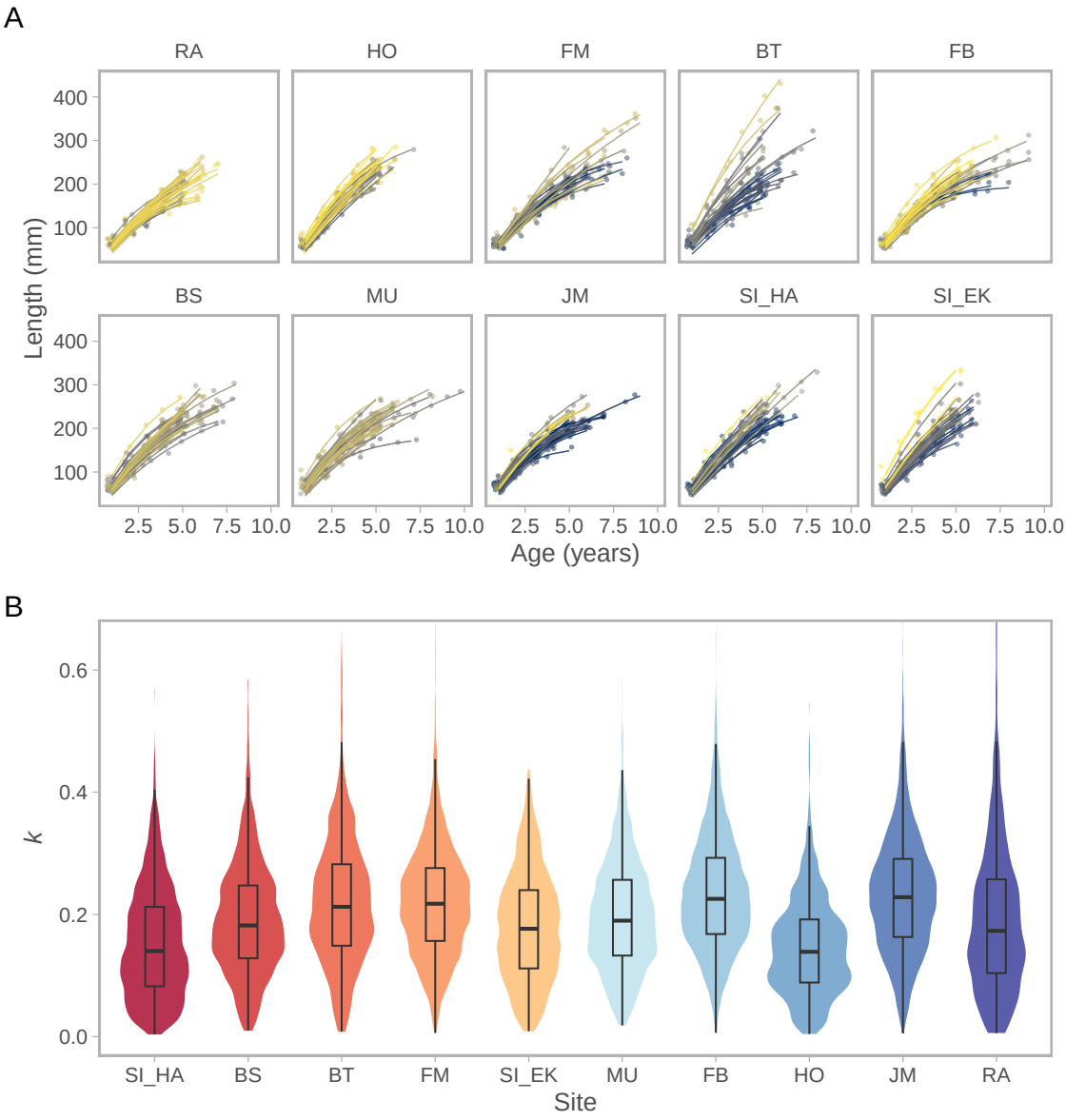

Figure 3: Length plotted against age for all sites (A). Points are data for 30 randomly selected individuals (indicated by colour) in each site, and lines are the predicted von Bertalanffy growth curve. Panel B depicts the distribution of von Bertalanffy growth coefficients k, where colours are based on the minimum temperature across all years, as violins, and quantiles depicted as boxplots.

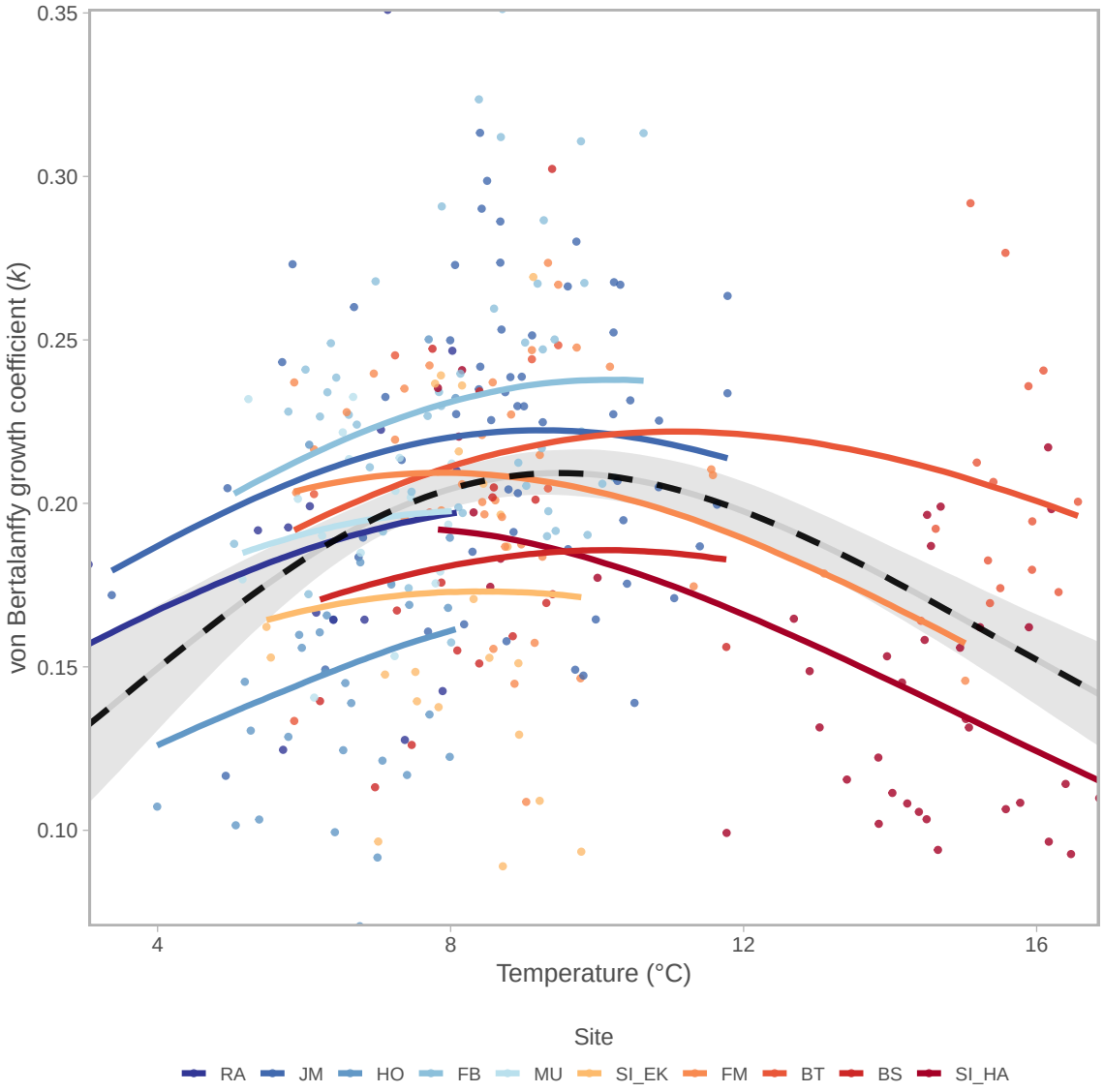

Figure 4: von Bertalanffy growth coefficients as a function of temperature. Each point depicts the median growth coefficient for a cohort and site, and the coloured lines depict the median of draws from the expectation of the posterior predictive distribution from the mixed effect Sharpe-Schoolfield model for each site. The black dashed lines depict the prediction from the pooled model. For uncertainty around site-specific predictions, see Fig. S5.

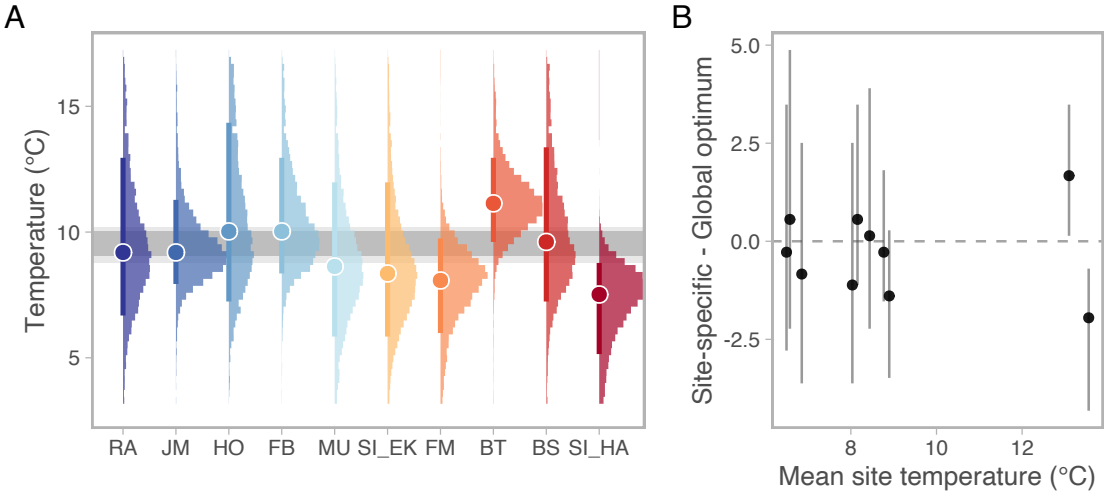

Figure 5: Ridgeplot depicting the distribution of site-specific optimum curves (temperature where the predicted growth coefficient is maximised) from the mixed effect Sharpe-Schoolfield model (A), and the deviation from the pooled optimum by site as a function of temperature (B). In panel A, the distributions of optimum temperatures are from 10.000 draws from the expectation of the posterior predictive distribution over the full temperature range. The horizontal dashed grey line depicts the optimum from the pooled Sharpe-Schoolfield model, and the grey rectangles indicate the 5^{th} and 95^{th} percentile (wide rectangle) and the 10^{th} and 90^{th} percentile (narrower rectangle) from the same distribution of draws. Points depict the median optimum temperature in that site, and the vertical lines are the 90% credible interval. Colours are based on the minimum temperature across all years. In panel B, the points indicate the difference between the median of the site-specific and the pooled model, and the vertical lines depict the difference between the 10^{th} and 90^{th} quantiles of site specific optima and the median of the pooled optimum.